25-033

Evaluating Roof Stability in an Underground Stone Mine Under High Horizontal Stress: Insight from Numerical Modeling and Field Observation with Mitigation Strategy

Gamal Rashed
CDC/NIOSH/PMRD

Nicole Evanek
CDC/NIOSH/PMRD

Tim Miller
East Fairfield Coal Company

ABSTRACT

High horizontal stress has been identified as a critical factor affecting roof stability in underground mines, particularly when the immediate roof consists of weak or laminated rock. Numerical models were employed to better understand the influence of caprock thickness, cutting sequences, and the orientation of driving direction relative to maximum horizontal stress on roof stability in underground stone mines. These models were calibrated based on field observations of roof falls from the study mine. The findings of this study enhance our understanding of roof stability under high horizontal stress and contribute to reducing the risk of roof falls in underground stone mines.

INTRODUCTION

There are currently 101 active underground stone mines in the United States (MSHA data retrieval system, 2023) where the room-and-pillar mining method is used to extract flat-lying and gently dipping formations. The stability of underground excavations depends on a combination of geological factors, the in-situ stress state, and operation-related-factors such as the size, shape, and orientation of openings, as well as the cutting sequence. The in-situ stress state, especially high horizontal stress, is a major factor contributing to roof instability in underground stone mines.

For horizontal, gravity-loaded roof beds clamped at both ends under a dominant vertical stress, failure typically initiates at the ends of the span (Obert and Duvall, 1967). The inclined stress trajectories at the ends of the beam direct the crack propagation diagonally (Goodman, 1989). When the roof span-to-bed thickness ratio exceeds 5.0, the failure mode is tension (Obert and Duvall, 1967). However, if horizontal stress becomes dominant, the failure mode shifts from tension to shear.

In mines in the eastern U.S., horizontal stress often exceeds vertical stress by a factor of at least two and can be even greater in shallow mines (Iannacchione et al., 1998; Iannacchione et al., 2001). Even though the overburden is shallow in some underground stone mines, horizontal stress levels can be unusually high due to tectonic plate movement, particularly the drift of the North American Plate from the Mid-Atlantic Ridge, and lead to significant horizontal stresses, even in regions with shallow overburden (Iannacchione et al., 2005; Esterhuizen and Iannacchione, 2005).

(Sheorey et al., 2001) proposed that horizontal stress is influenced by elastic constants, overburden depth, and the coefficient of thermal expansion based on stress measurements. Similarly, Mark and Gadde (2010) analyzed over 350 stress measurements and concluded that the magnitude of the maximum horizontal stress can be determined using both depth and the modulus of elasticity.

The impact of high horizontal stress on roof stability and the development of cutter failure in underground coal mines has been extensively studied by numerous researchers (Jeremic, 1981; Gale and Blackwood, 1987; Mucho and Mark, 1994; Wang and Stankus, 1998; Chen, 1999; Gadde and Peng, 2005; Peng, 2007). However, there is limited literature addressing the effects of high horizontal stress on roof stability in hard rock mines. Hence, the conclusions and findings drawn from studies of high horizontal stress in coal mines may not be applicable to stone mines due to significant differences in rock strengths, roof spans, mining heights, geological conditions, and in-situ stress conditions between hard rock and coal mines.

High horizontal stress can significantly impact roof stability in underground stone mines, leading to roof fall and hazardous conditions. Managing and alleviating the effects of high horizontal stress is crucial for mine safety. The presence of high horizontal stress is evident through various failure patterns, including cutter failure, elliptical roof failure oriented perpendicular to the direction of maximum horizontal stress, and low-angle shear failure. Geological mapping of horizontal stress failure patterns can help identify the orientation of the maximum horizontal stress. (Iannacchione et al., 2020).

Cutter failure refers to the damage of roof layers, typically near the rib, caused by horizontal compression. This can lead to roof failure. Cutter failure can lead to roof falls if no proper and timely measures are implemented to prevent their continuing development (Peng, 2008). The characteristic signs of high horizontal stress are generally considered stress driven. However, some researchers have suggested that other factors, such as the mechanical properties of the rock and the relative stiffness of different rock types, may also contribute to cutter failure (Ray, 2008). Over the years, underground mines have employed various strategies to mitigate the detrimental effects of high horizontal stress. These strategies include the use of primary and secondary roof support, aligning headings in favorable directions, and reducing the number of crosscuts (Iannacchione et al., 2020).

This study presents the results of FLAC3D numerical models and field observations conducted at the Subtropolis Mine to investigate the effects of high horizontal stress on roof stability. The primary objective of this study is to explore the interaction between caprock thickness and the orientation of maximum horizontal stress on roof stability. The impact of the cutting sequence on roof stability was also examined, and a few straightforward recommendations are provided to mitigate such instabilities. The underlying assumption of this study is that high horizontal stress in the limestone formation is high enough to trigger failure in the roof rock mass after development. In this paper, the terms "Headings" and "Entries" are used interchangeably. Headings/Entries refer to the direction of mining into the reserve.

HIGH HORIZONTAL STRESS AND ROOF RESPONSE AT SUBTROPOLIS MINE

Many underground stone mines in the U.S. are adversely affected by high horizontal stress, with the Subtropolis room-and-pillar mine being a notable example. The Subtropolis Mine exhibits several characteristic signs of high horizontal stress conditions. Geological mapping has confirmed the presence of floor heave/failure (see Figure 1),

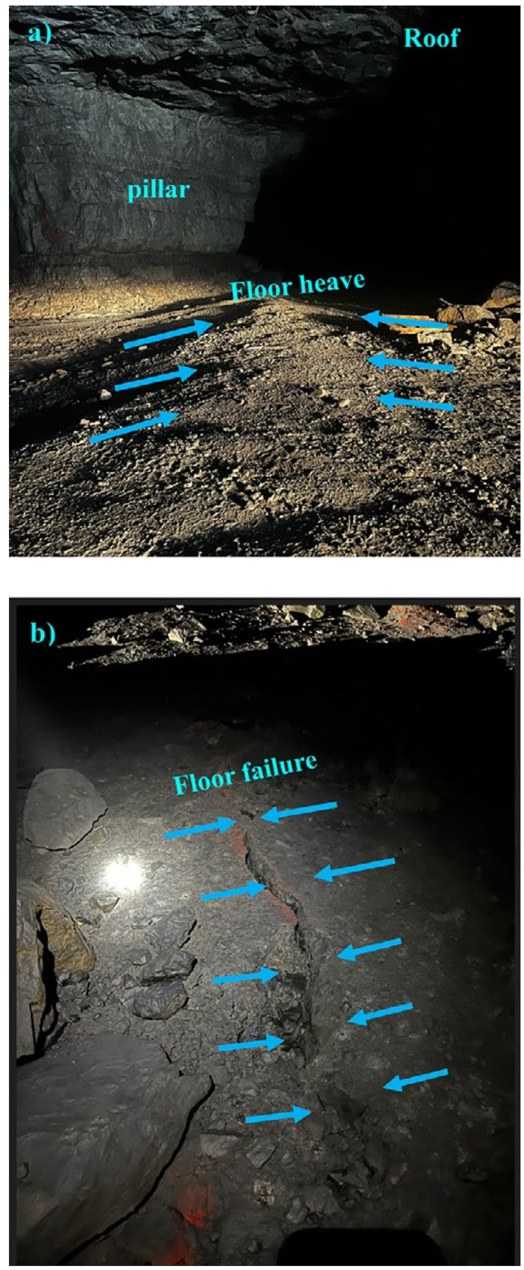

Figure 1. Floor heave and failure observed at Subtropolis Mine caused by high horizontal stress. The affected floor rock is limestone

cutter roof failure (see Figure 2), sporadic roof shearing, progressive directional roof falls, and immediate roof separation and shifting along with sheared bolts (see Figure 3).

This study was conducted at Subtropolis Mine, which extracts the Vanport Limestone, which is part of the Allegheny Formation within the Pennsylvanian System. The limestone ranges in thickness from 16 to 22 ft (4.9 to 6.7 m), with a mining height of approximately 16 ft (4.9 m) and a roof span between 30 and 40 ft (9.1 and 12.2 m) (Iannacchione et al., 2020).

The primary roof support pattern at this mine consists of five, 5 ft (1.5 m) long fully grouted combination resin

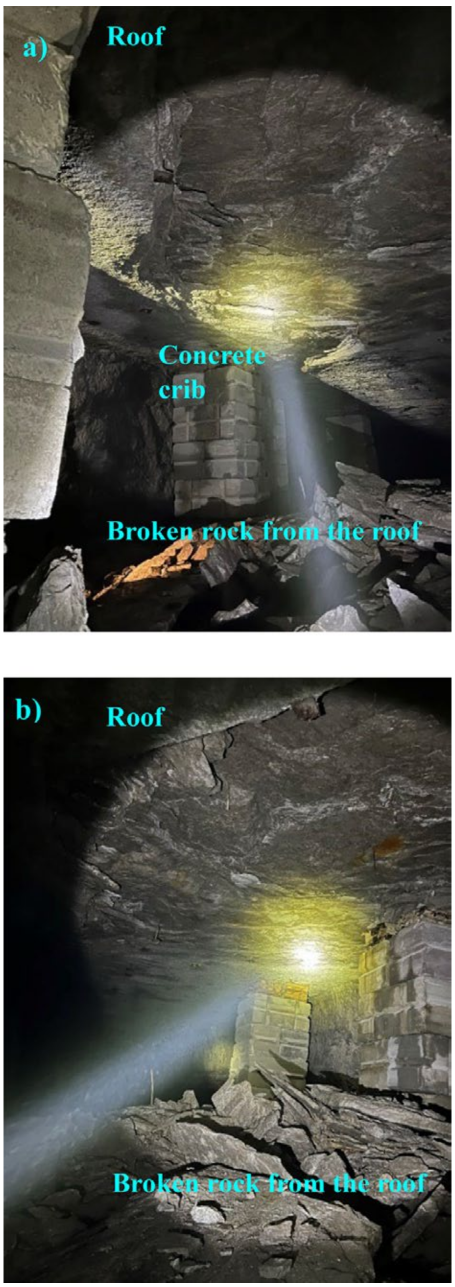

Figure 2. Cutter failure along the rib resulted in roof fall

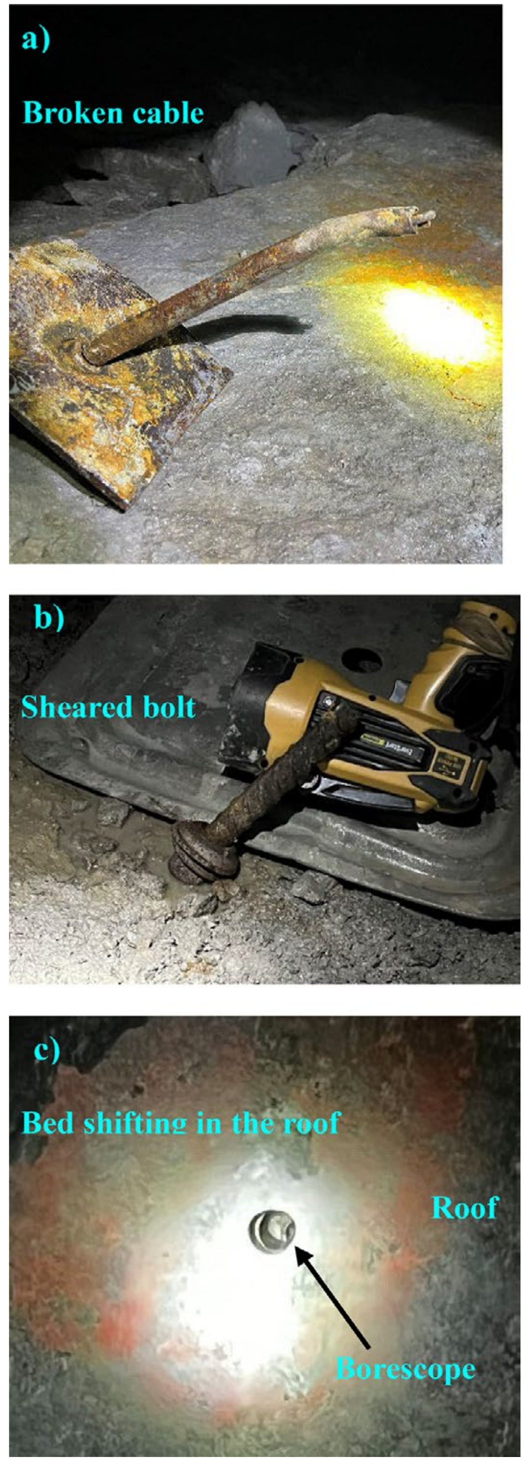

Figure 3. Broken cable, sheared bolt, and roof bed shifting due to high horizontal stresses

bolts to a row, 8 ft (2.4 m) apart, with 8 ft (2.4 m) between each row. The secondary roof support pattern includes 8 ft (2.4 m) long fully grouted cable bolts, four bolts per row, spaced between the primary fully grouted bolts.

The secondary roof support pattern is routinely used in crosscuts and within the headings adjacent to crosscuts (Evanek, et al., 2020). The floor rock at the study mine is limestone, with a thickness ranging from 1 to 2 ft (0.3 to 0.6 m), underlain by sandstone. However, in the western region of the mine, a layer of fireclay is present between the limestone and the sandstone.

Limestone specimens from the study mine (Vanport Limestone Formation) were tested under both uniaxial and triaxial conditions. As summarized in Table 1, The tested specimens had a length-to-diameter ratio of nearly 2.0, with a diameter of approximately 2.0 inches (5.0 cm). The unconfined compressive strength ranged from 18,270 to 19,720 psi (126 to 136 MPa), and the estimated friction angle derived from the triaxial test results was about 45°. Additionally, direct shear tests were performed on saw-cut limestone specimens from the study mine to determine the internal friction angle. The friction angle from the direct shear tests varied between 21° and 30°, depending on the choice of the inflection point where the slope of the shear stress versus shear displacement curve changes. These material properties were used to generate the FLAC3D models to explore the effect of horizontal stress on roof stability.

Given the shallow overburden at the study mine, less than 150 ft (45.7 m), the horizontal stress levels must be sufficiently high to cause failure in such strong roof rock. The direction of the maximum horizontal stress at the mine was determined based on the pattern of roof cutters and falls, with the predominant direction trending toward N35W. However, stress mapping of roof damage shows that the orientation of the maximum horizontal stress varies across different areas of the mine. As a result, the mine has had to repeatedly adjust the orientation of headings to mitigate the adverse effects of high horizontal stress as shown in Figure 4 (Evanek et al., 2024).

Table 1. Laboratory test results for uniaxial and triaxial tests on limestone specimens from the Vanport formation

Specimen #	Length/ Diameter	σ3, MPa	σ1, MPa	Tangent mod, MPa
1	1.94	0	136	24,500
2	1.95	0	126	45,100
3	1.95	3	141	64,800
4	1.95	6	136	57,400
5	1.94	8	171	NA
6	1.96	14	204	48,300
7	1.97	17	225	72,500
8	1.97	11	204	NA

The mine operator has diligently experimented with different techniques/methods to lessen the impact of the instabilities in the outby crosscuts. The range of controls used by the mine operator include, angled crosscuts, crosscut offsets, increase distance between crosscuts, arched crosscuts, cable bolted crosscuts, altered blasting pattern, and windows. A window is used to resist roof deformation by leaving a strong brow of roof rock within the crosscuts (Evanek, et al., 2020).

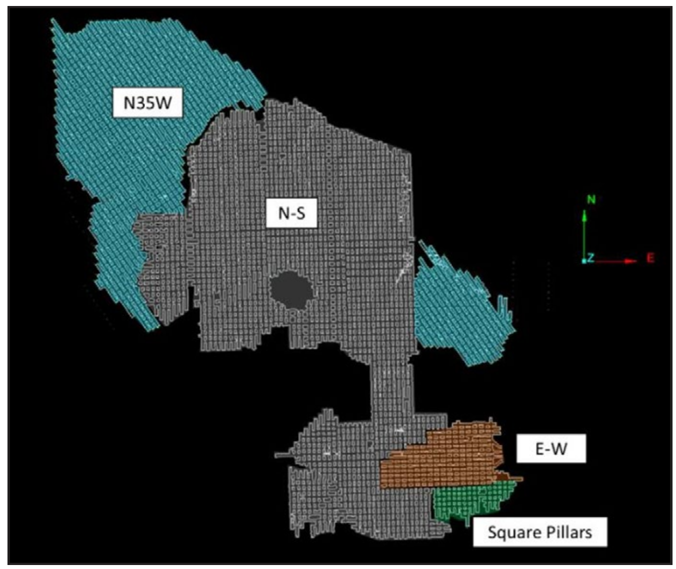

Figure 4. Subtropolis Mine map with varying heading orientations (after Evanek et al., 2024)

EFFECT OF MAXIMUM HORIZONTAL STRESS ORIENTATION ON ROOF STABILITY

The impact of maximum horizontal stress orientation on roof stability was investigated using FLAC3D models. Several models were developed to simulate two entries and a crosscut under high horizontal stress. The entry width was set at 40 ft (12.2 m), the crosscut at 30 ft (9.1 m), with a mining height of 16 ft, and a cover depth of 130 ft (39.6 m). These input parameters reflect the mining conditions at the study mine. In all models, the maximum horizontal stress was aligned with the Y-direction, while the mine geometry rotated at an angle (θ), as shown in Figure 5. The angle θ varied from 0 to 90 degrees in 15-degree increments. The excavations were modeled in a uniform, elastic rock mass with an interface between the caprock and the main roof.

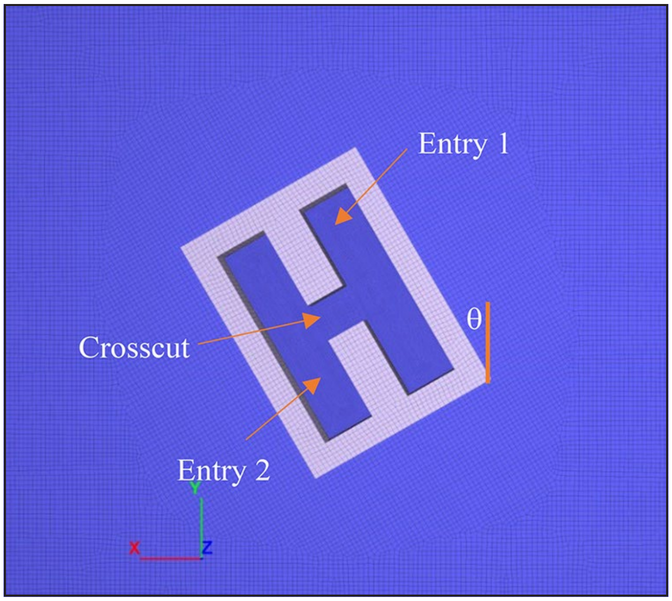

Figure 5. Plan view of the FLAC3D model geometry. The mine geometry is rotated by an angle q relative to the maximum horizontal stress, which is aligned with the Y-axis

The mechanical properties of the caprock (limestone) and the main roof (shale) are summarized in Table 2. To evaluate the effect of the maximum horizontal stress angle on entry and crosscut stability, the safety factor was calculated at different roof elevations (6 inches and 2 ft (0.61 m) from the roofline). The strength of roof elements was estimated using the Hoek-Brown strength criterion, while induced stresses were obtained from the FLAC3D models. The failure percentage was calculated as the ratio of elements with a safety factor below 1.0 to the total number of elements.

The FLAC3D model dimensions are 498.6 ft × 505.1 ft × 226.3 ft (152 m × 154 m × 69 m) in the X, Y, and Z directions, respectively. The model was solved in four steps: first, the geostatic step to initialize the in-situ stresses; second, the development of Entry 1; third, the excavation of the crosscut; and lastly, the development of Entry 2. The *zone relax excavate* command in FLAC3D was used to simulate the excavation process and mitigate unrealistic results caused by the sudden removal of rock material. The model boundaries were constrained to move only in the vertical direction, while the bottom was fixed in the X, Y, and Z directions. The immediate roof at the study mine consists of limestone, with a thickness ranging from 2 to 8 ft (0.61 to 2.4 m). This limestone layer is overlain by shale, which forms the main roof. An interface is assumed between the limestone and shale, with its properties listed in Table 3. Both the shale and the limestone are considered massive and free from geological discontinuities.

Table 2. Summary of the geotechnical parameters used in the model

Rock Type	Parameter	Value
Immediate roof (limestone)	Unconfined compressive strength, (MPa)	110
	Poisson's ratio	0.20
	Intact Young's Modulus, (GPa)	45.5
	Hoek-Brown m_i Parameter	9.98
	Hoek-Brown s Parameter	1.0
	Geological strength index (GSI)	70
Main roof (shale)	Intact Young's Modulus, (GPa)	22.5
	Poisson's ratio	0.25

Table 3. Mechanical properties for the interface used in the model

Parameter	Value
Normal stiffness, MPa/m	13,000
Shear stiffness, MPa/m	2,600
Friction angle, degree	20.0
Friction-residual, degree	12
Cohesion, MPa	0.50
Cohesion-residual, MPa	0.1
Tension, MPa	0.1
Tension-residual, MPa	0.05

Figure 6 illustrates the variation in failure percentage in the caprock of Entry 1 and the crosscut under different orientations of maximum horizontal stress, with a caprock thickness of 2 ft (0.61 m). The failure percentage is minimal when the maximum horizontal stress is aligned or nearly aligned with the entry direction. In contrast, the failure percentage is highest when the stress is perpendicular or nearly perpendicular to the entry. Since the crosscut is perpendicular to the entry as shown in Figure 5, the optimal orientation for minimizing failure in the entry leads to the worst performance in the crosscut, and vice versa.

Before mining, the maximum stress in the roof was around 1,595 psi (11 MPa). After mining, if the heading was aligned perpendicular to the maximum horizontal stress, it caused significant disturbance in the stress field, as illustrated in Figure 7a. The maximum stress in the roof increased to more than double over the excavated area, while the stress in the unmined roof near the middle of the excavation at the sides decreased by nearly half, creating a relief zone. In contrast, aligning the heading parallel to the maximum horizontal stress resulted in minimal disturbance in the stress field, leading to more stable conditions for the roof, see Figure 7b.

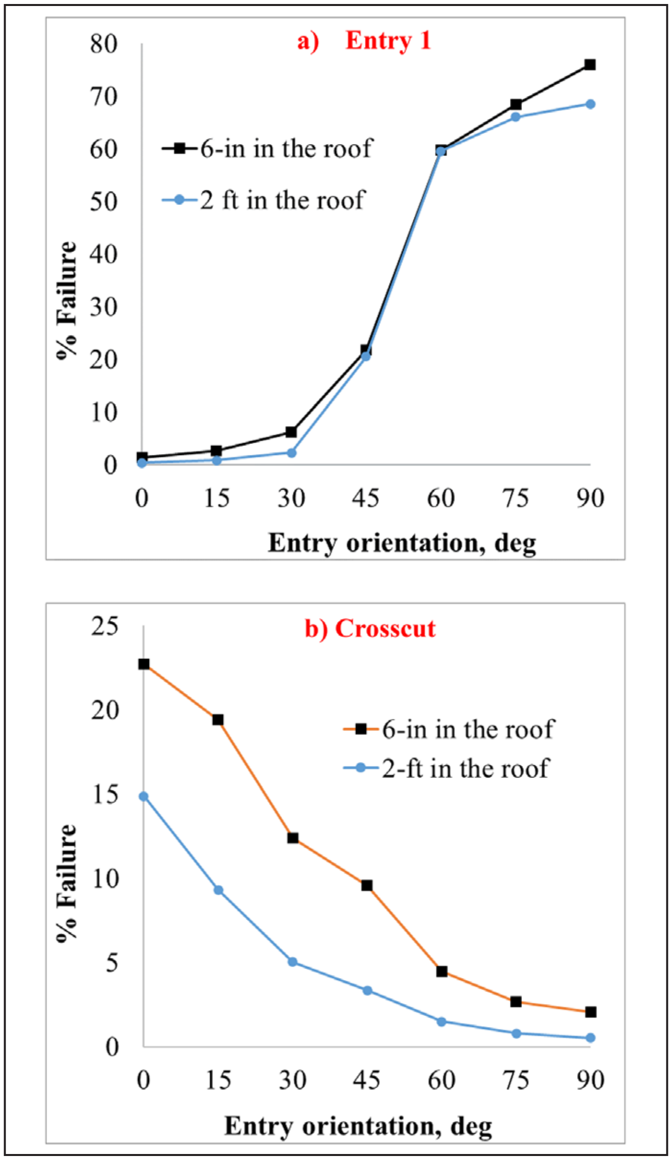

Figure 6. Variation of percent roof failure with maximum horizontal stress orientation for a) Entry 1 and b) Crosscut based on FLAC3D elastic models. The caprock thickness is 2 ft (0.61 m)

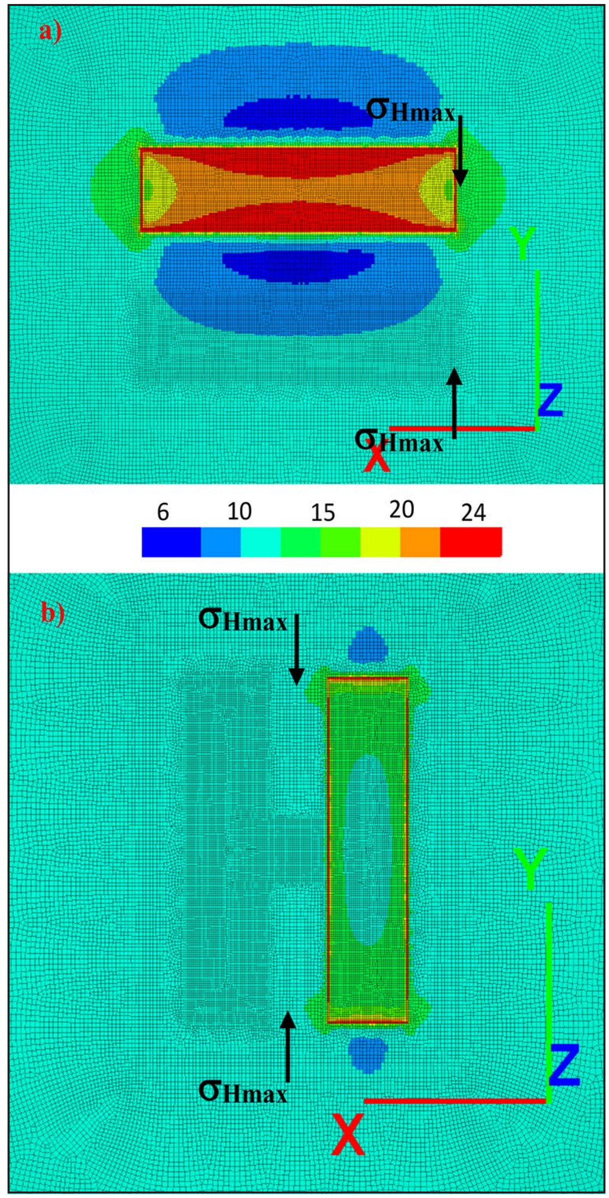

Figure 7. Distribution of maximum principal stress (s1) in the roof of Entry 1: a) when Entry 1 is oriented perpendicular to the maximum horizontal stress and b) when Entry 1 is oriented parallel to the maximum horizontal stress. Stress values are in MPa. Note that Entry 2 and the Crosscut have not been mined yet

CUTTER FAILURE INITIATION AND DEVELOPMENT

Cutter roof failure is primarily attributed to shear stress at the entry corner exceeding the shear strength of the rock. Figure 8 illustrates the shear stress distribution in the immediate roof above Entry 1 at 0°, 30°, and 90° orientations from FLAC3D models. Note that Entry 2 and the Crosscut have not been mined yet.

At 0° orientation, the maximum shear stress is concentrated at the face, indicating that failure would likely occur there. In contrast, at 90° orientation, shear stress peaks at the sides and is lowest at the face, suggesting that failure is expected to happen at the sides. The shear stress at 90° orientation is significantly higher than at 0°. At a 30° orientation, one corner experiences a higher shear stress concentration compared to the other corner, indicating that failure would initiate at that corner and propagate along both the face and the side near the stressed corner.

Roof cutter failure is a progressive phenomenon driven by shear failure, which initiates at the intersection of the

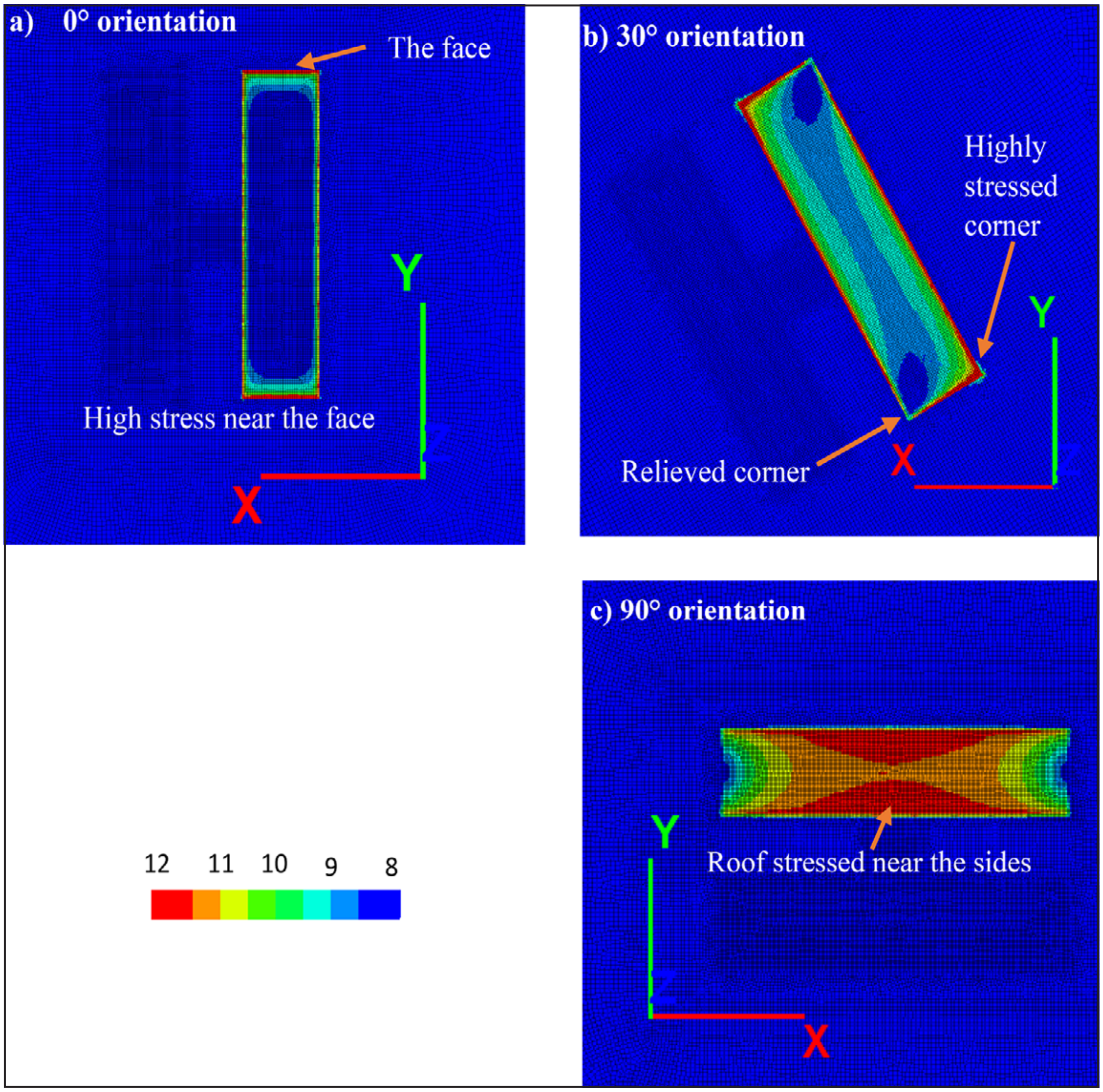

Figure 8. Shear stress distribution in the immediate roof, with values in MPa, at 0°, 30°, and 90° orientations, the maximum horizontal stress aligned along the Y-axis

roofline and the pillar. Cutter failure can lead to roof falls, with the time between the cutter failure and the roof fall ranging from a few weeks to years. The cutter damage appeared to zig-zag vertically in thinner beds and more horizontally in thicker ones (see Figure 9). Simple numerical models indicate that cutter failure will stop propagating through the roof if a gap or separation occurs between roof beds.

Field observations revealed that bolts in the center of the cutter (shear zone) exhibited tensile failure, with clear cup-and-cone fractures. In contrast, bolts farther from the center experienced shear failure. This suggests that bed separation occurs near the center of the cutter (shear zone).

In an ideal scenario with symmetric loading conditions and a uniform, homogeneous rock mass across the entry/heading, cutter failures would propagate at both corners of the entry when the maximum horizontal stress is perpendicular to it, as shown in the schematic in Figure 10. However, in practice, as observed at the study mine, cutter failure typically propagates along one side due to asymmetrical material properties, uneven loading conditions, or more pronounced geological discontinuities on one side of the heading.

The cutter failure observed at the study mine differs from that typically seen in underground coal mines. In coal mines, cutter failure often occurs near the rib with an almost vertical orientation. In contrast, cutter failure in stone mines exhibits a zig-zag pattern, see Figure 9. This discrepancy is likely due to differences in roof strength and lamination thickness. In coal mines, cutters usually form in

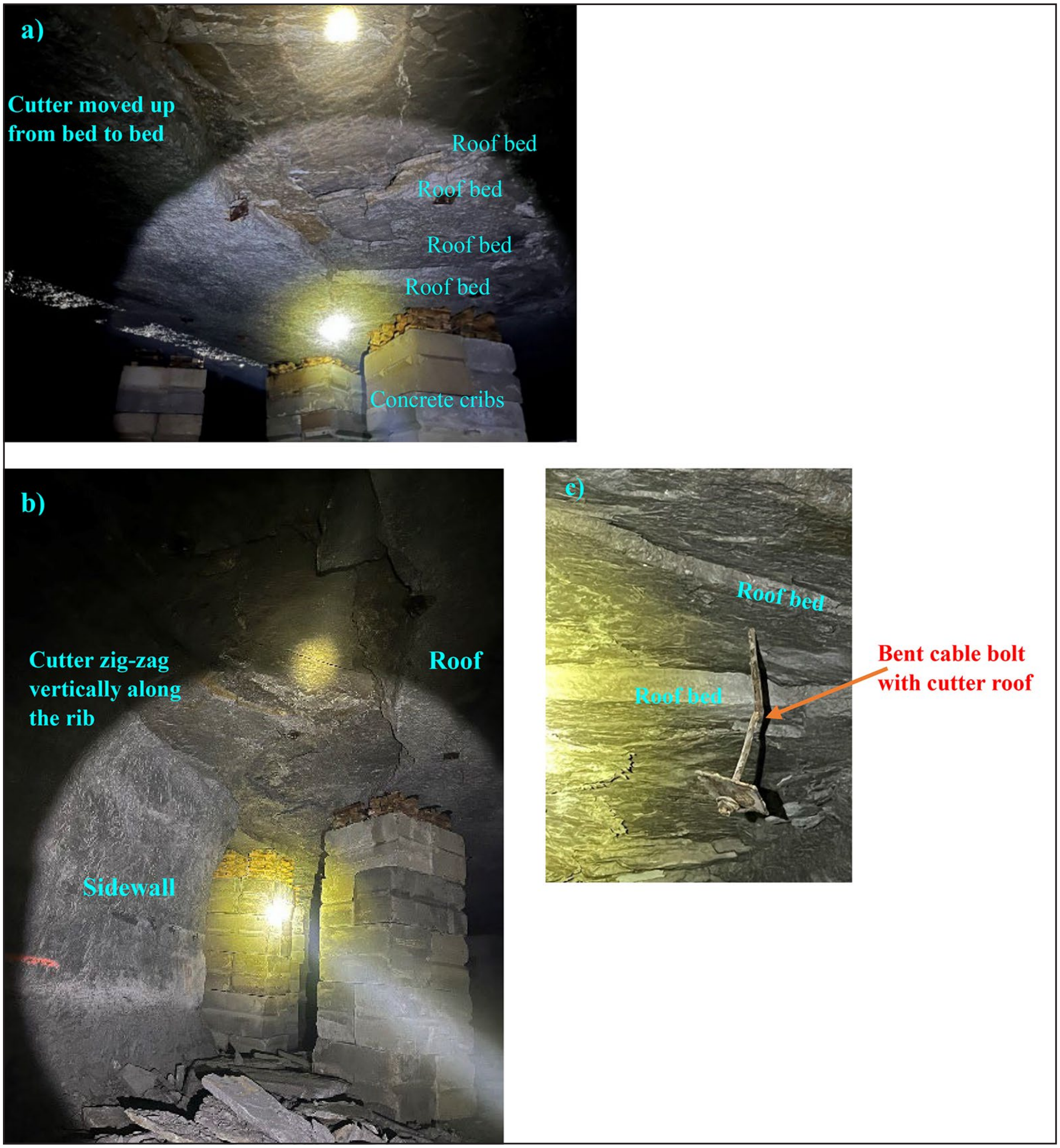

Figure 9. Cutter propagation in a zig-zag pattern between roof beds

softer rocks, such as shale and claystone, with thin laminations. In stone mines, however, cutters occur in harder rock, like limestone, with thicker laminations. Consequently, softer rocks with thinner laminations tend to produce vertical cutters, as seen in coal mines, while harder rocks with thicker laminations lead to the zig-zag cutter pattern observed at the study mine.

According to Mohr Coulomb theory, fracture takes place through the direction of the intermediate principal stress and inclined at an angle less than 45 degrees from the direction of the maximum principal stress (Jaeger et al., 2007). The fracture angle is the angle between the shear fault plane and the axis of the maximum principal stress. The maximum shear stress angle can shift depending on the horizontal to vertical stress ratio and the magnitude of the shear stress. The fracture angle increases with increasing $\sigma 3$, but decreases with increasing $\sigma 2$, particularly under lower $\sigma 3$ values (Mogi, 2007).

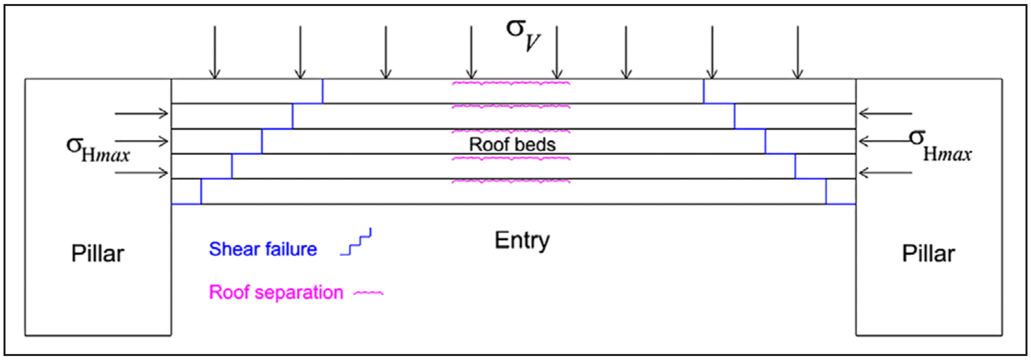

Figure 10. Schematic for the zig-zag pattern for the development of cutter roof failure at the study mine, σ_V is the vertical stress, and σ_{Hmax} is the maximum horizontal stress.

Accumulated field data over several months revealed a distinct pattern: broken bolts were found almost daily in one area, followed by months of inactivity, after which similar failures occurred elsewhere in the mine, aligned with the direction of the cutter failure. This recurring pattern allowed the mine operator to better anticipate future cutter failures.

As illustrated in Figure 11, broken bolts, roof cracking, and roof shear are mapped. The cutter, which developed in February (dates shown in red), caused multiple bolts to shear through February and March, followed by a quiet period in April and May. In June, a few broken bolts, roof cracks, and cutter activity were observed, with no activity in July. The pattern resumed in August and September, with roof cracking and cutter shearing.

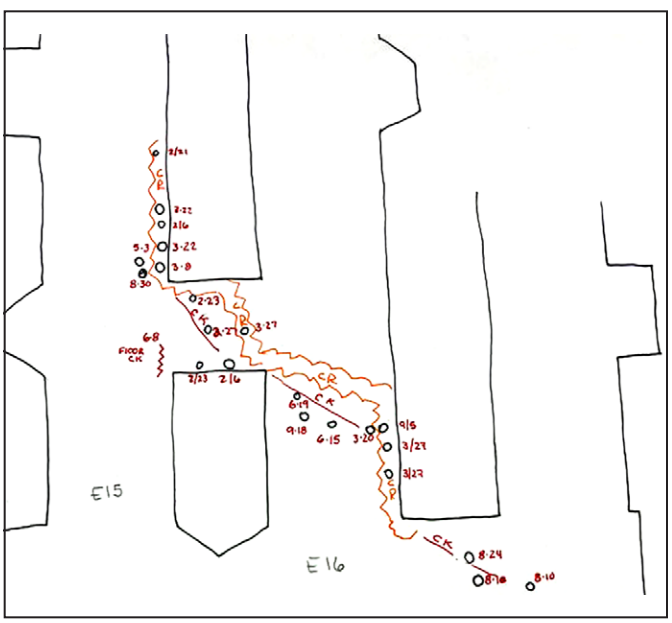

Figure 11. Schematic illustrating the timing of roof bolt shearing and cutter development based on accumulated field data collected over several months

The ⅞-inch Grade 60 bolt used for roof support in the mine would require a differential displacement of approximately 0.0048 inches (0.12 mm) between the roof beds to shear and break, assuming a shear length of 1 inch due to roof separation.

3D LIDAR SCAN TO CAPTURE CUTTER FAILURE AND ROOF FALLS

Figure 12 confirms the roof damage and orientation observed in the mine using 3D LiDAR scanning. Scans were taken in the same entries shown in Figure 11, validating the field observations. The point clouds were captured using the Maptek I-Site 8200 stationary scanner at approximately 50 ft intervals. These point clouds were registered and colored from an estimated roof line (in white), with damage highlighted in red to indicate higher roof elevation. Both Figures 11 and 12 show that cutter failures are oriented along the right rib of Entry 15, suggesting that the principal horizontal stress in this area of the mine is

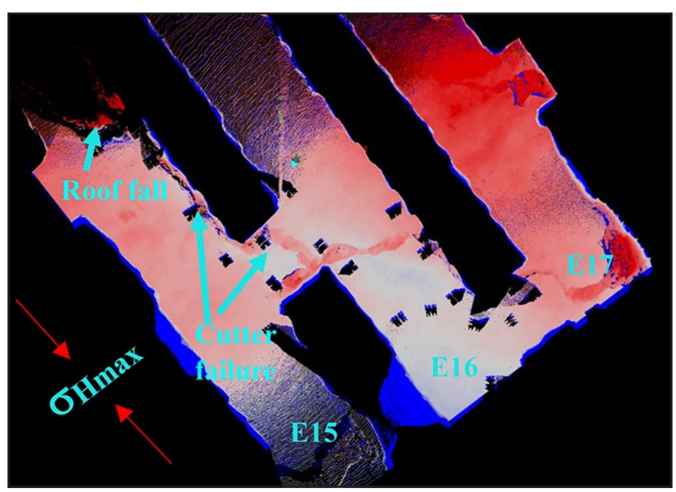

Figure 12. 3D LiDAR scans of the roof in the same entries as Figure 11, showing cutter development, with red indicating higher roof elevations or areas of roof damage

approximately N35W. The figures also illustrate that the cutter failure propagates along one side of the entry, resulting from uneven loading conditions due to horizontal stress.

EFFECT OF CAPROCK THICKNESS ON ROOF STABILITY

The caprock thickness refers to the unmined portion of the limestone formation left in the roof during development. This thickness plays a crucial role in roof stability in underground stone mines, particularly when subjected to high horizontal stress based on field experience. To evaluate the interaction between the orientation of maximum horizontal stress and caprock thickness on roof stability, FLAC3D models were employed to simulate three different caprock thicknesses— 2 ft (0.6 m), 4 ft (1.2 m), and 8 ft (2.4 m)—across various orientations. The caprock is essential in supporting the main roof at Subtropolis Mine, which primarily consists of weak shale. If the caprock fails, it can lead to progressive failure extending into the main roof, increasing the risk of roof falls.

As illustrated in Figure 13, model results show that with an 8-ft (2.4 m)thick caprock, the percentage of failure remains significantly lower, even at the most unfavorable orientation (90°), compared to the 2-ft (0.6 m) thick caprock scenario. These results align with field observations at the study mine, where thicker caprock (around 8 ft or 2.4 m) helps mitigate the impact of maximum horizontal stress on roof stability. On the other hand, when the caprock is thinner (less than 4 ft or 1.3 m), the orientation of maximum horizontal stress becomes a critical factor, significantly influencing roof stability.

To alleviate the effects of high horizontal stress, the mine adopted a strategy of aligning headings parallel to the maximum horizontal stress and creating "window" crosscuts. A window is created by leaving a thicker section of roof rock in the crosscuts, which reduces the vertical dimensions of the crosscuts. This method lowers the mining height while maintaining the caprock thickness approximately 4 ft (1.3 m) higher than the heading. Additionally, the operator opted to offset these windows to limit the propagation of stress damage within the crosscuts. Evanek et al. (2020) provide detailed information on the utilization of windows to control crosscut damage caused by high horizontal stress. This method reduces the mining height and maintains the caprock thickness about 4 ft (1.2 m) higher than the heading. This approach enhances stability: the headings are more stable due to their parallel alignment with the maximum horizontal stress, while the crosscuts benefit from the thicker caprock, which effectively redistributes stresses and reduces shear stress concentrations in the immediate roof.

When the caprock is thin, shear stress in the roof across the excavation is higher, as shown in Figure 14, compared to thick caprock. This increases the likelihood of roof falls since thin caprock cannot effectively redistribute the induced stresses from the excavation. Instead, it concentrates them due to its higher stiffness relative to the main roof. Thin caprock not only concentrates more stress in the immediate roof but also experiences greater deformation, making the roof less stable compared to thick caprock. Based on the FLAC3D model under identical conditions,

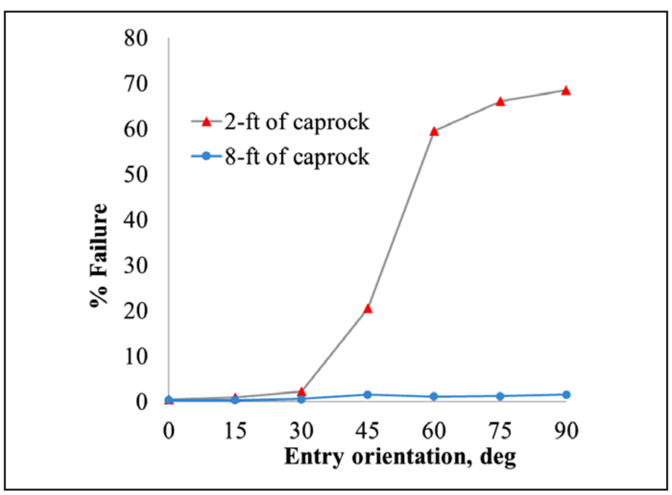

Figure 13. Percentage roof failure from the FLAC3D models for both thick and thin caprocks under high horizontal stress

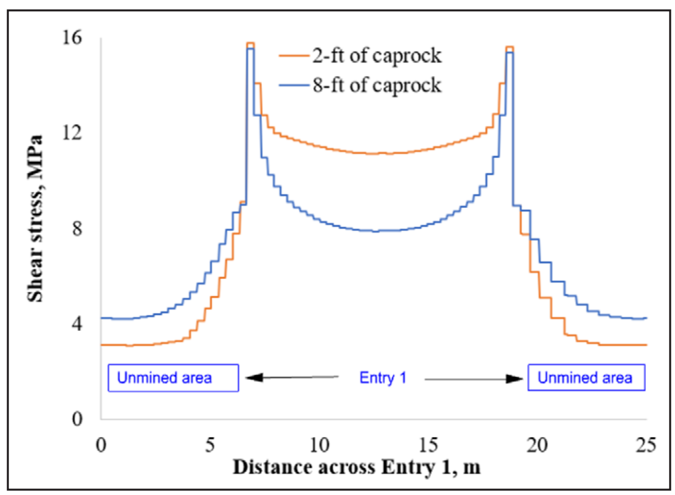

Figure 14. Shear stress distribution across Entry 1 at 90° orientation, 6 inches from the roofline, from the FLAC3D model for thick and thin caprocks under high horizontal stress. Refer to Figure 5 for the location of Entry 1

the displacement magnitude at the center of the excavation for the 2-ft (0.61 m) caprock was about five times greater than that of the 8-ft (2.4 m) caprock.

Evanek et al. (2024) identified five key indicators to predict potential instability zones at the study mine, the likelihood of instability increases when multiple indicators are present at a given location. These indicators include:

1. Heading Orientation: North-South headings experienced more roof failures.
2. Overburden Depth: Depths exceeding 140 ft (42.7 m) were flagged as high-risk.
3. Caprock Thickness: Thicknesses below 3 ft (0.9 m) were considered hazardous.
4. Proximity to Stream Beds: Areas within 200 ft (61.0 m) posed increased risk.
5. Proximity to Joints and Clay Veins: Areas within 100 ft (30.5 m) were flagged.

Table 4. Summary of strain-softening material model used in FLAC3D

Rock type	Parameter	Value
Immediate roof (limestone)	Cohesion, MPa	7.5
	Poisson's ratio	0.20
	Friction angle, degree	30
	Dilation angle, degree	10
	Cohesion softening table: (0,7.5) (0.004, 2.0) (0.01, 1.7)	
	Friciton softening table: (0,30) (0.0005, 15) (0.01, 12)	
Main roof (shale)	Cohesion, MPa	3.5
	Poisson's ratio	0.20
	Friction angle, degree	25
	Dilation angle, degree	10
	Cohesion softening table: (0,3.5) (0.001, 1) (0.02, 0.2)	
	Friciton softening table: (0,25) (0.0005, 15)	

EFFECT OF FACE ADVANCE METHOD ON ROOF PERFORMANCE UNDER HIGH HORIZONTAL STRESS

Recognizing and assessing the stability of a mine roof is a crucial practice that has been adopted by many underground stone mines to prevent roof falls and ensure the safety of workers. The Subtropolis Mine has tested various ground control strategies to reduce stress concentrations in the roof caused by high horizontal stress during face advance. One key strategy involved identifying the most effective face advance method to improve roof stability. The roof performance and associated roof falls were evaluated for two face advance methods—flat-front and arrowhead. In the flat-front method, all faces advance simultaneously, while the arrowhead method staggers them in an arrow shape.

The FLAC3D models, utilizing a strain-softening material model (see Table 4 for properties), were employed to explore the impact of horizontal stress on roof stability for flat-front and arrowhead advance methods. The nonlinear material model was used in this section through to the end of the paper, rather than the elastic material model, because interactions between entries can relieve induced stresses in the roof. Using an elastic material model may therefore produce unrealistic results. In the previous section, however, the elastic model was appropriate because only a single entry was excavated at various orientations. Additionally, when an entry and a crosscut were excavated, the interaction between them did not relieve the induced stresses in the roof. Therefore, justifying the use of the elastic model.

Figure 15 illustrates cutter failure based on field observations. The cutter failure depicted in Figure 15 highlights the location of failure due to high horizontal stress but does not account for the magnitude of the damage or failure.

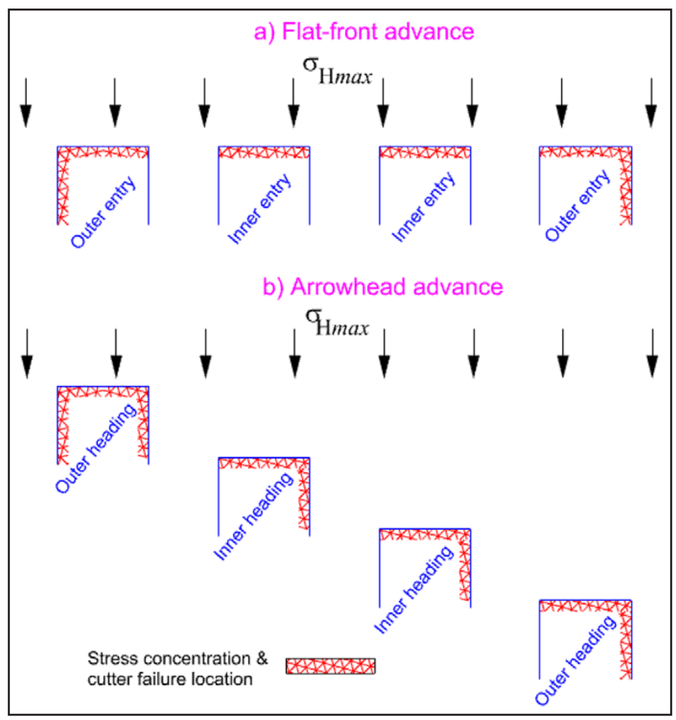

Figure 15. Schematic representation of cutter failure for a) flat-front mining and b) arrowhead mining in advancing headings, where the high horizontal stress is parallel to the driving direction. This schematic does not consider the magnitude of damage

The FLAC3D models suggest that cutter failure primarily impacts the roof at the face when using the flat-front cutting method. However, with the arrowhead cutting method, high horizontal stress affects both the face and the sides of the unmined side, as illustrated in Figure 16. Based on field observations and model results, it is recommended to advance the face using the flat-front method when the roof is subjected to high horizontal stress.

When the maximum horizontal stress is perpendicular to the headings, outer headings experience more yield than inner ones, as illustrated in Figure 17. This figure depicts the yield pattern from the FLAC3D model. In the flat-front method, cutter failure occurs in the roof at the sidewall locations while the face remains unaffected. In contrast, the arrowhead method results in failure at both the front face and the unmined sidewall, with significantly higher failure magnitudes.

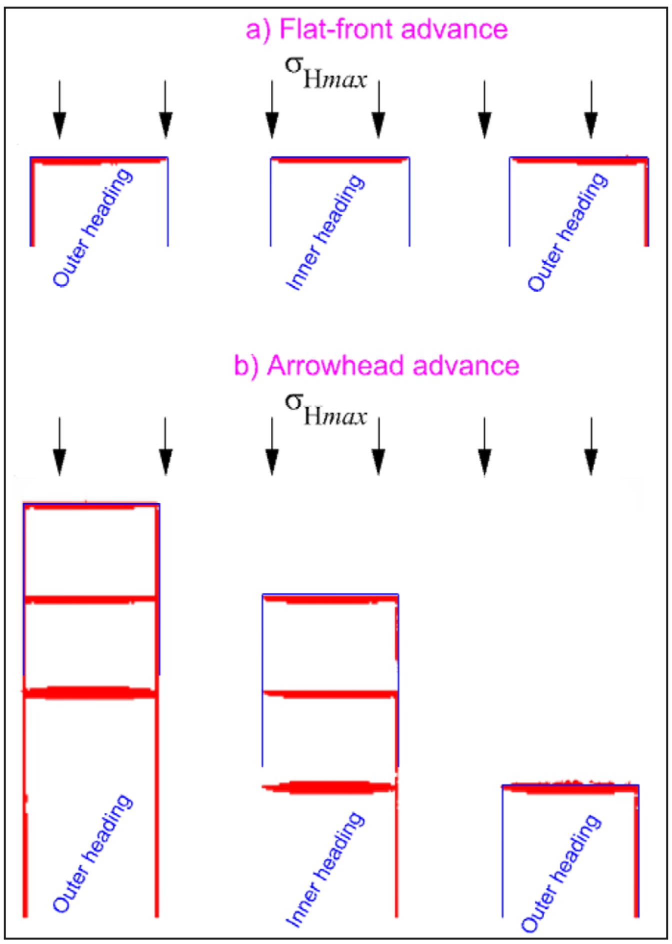

Figure 16. Yield patterns from the strain-softening FLAC3D model for (a) flat-front mining and (b) arrowhead mining in advancing headings. Red areas indicate zones of yielding

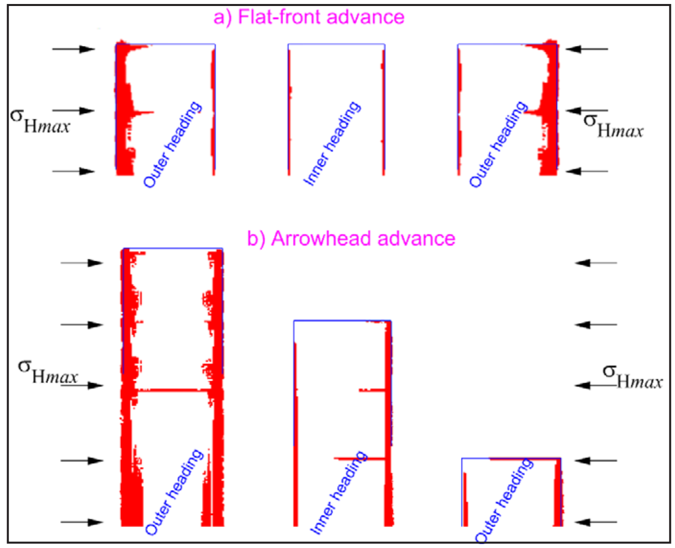

Figure 17. Yield patterns for flat-front and arrowhead advance based on the FLAC3D model, with yielded regions highlighted in red when the maximum horizontal stress is perpendicular to the headings

EFFECT OF CROSSCUT DEVELOPMENT METHODS ON ROOF STABILITY

At Subtropolis Mine, two methods are used for crosscut development:

1. **Method 1:** A crosscut is developed from an existing entry, then the newly developed crosscut is used to create another entry. In this case, the crosscut becomes longer as it includes both the length of the crosscut and the width of the newly developed entry. The rock in the extended crosscuts requires four cuts for excavation. The encircled numbers indicate the cutting sequence, as illustrated in Figure 18: Entry 1 was excavated in cut 1, the crosscut was excavated in cuts 2, 3, 4, and 5, and Entry 2 was excavated in cut 6.
2. **Method 2:** A crosscut is developed by connecting two existing entries. the rock in the crosscut is excavated in two cuts. Entry 1 was excavated in cut 1, Entry 2 was excavated in cut 2, and the crosscut was excavated in cuts 3 and 4.

The stability of a newly developed crosscut (Method 1 versus Method 2) was analyzed using a numerical model, with results validated against field observations. The thickness of the caprock used in these models is 4 ft (1.2 m). There was strong agreement between the field observations and the FLAC3D model results. It was found that

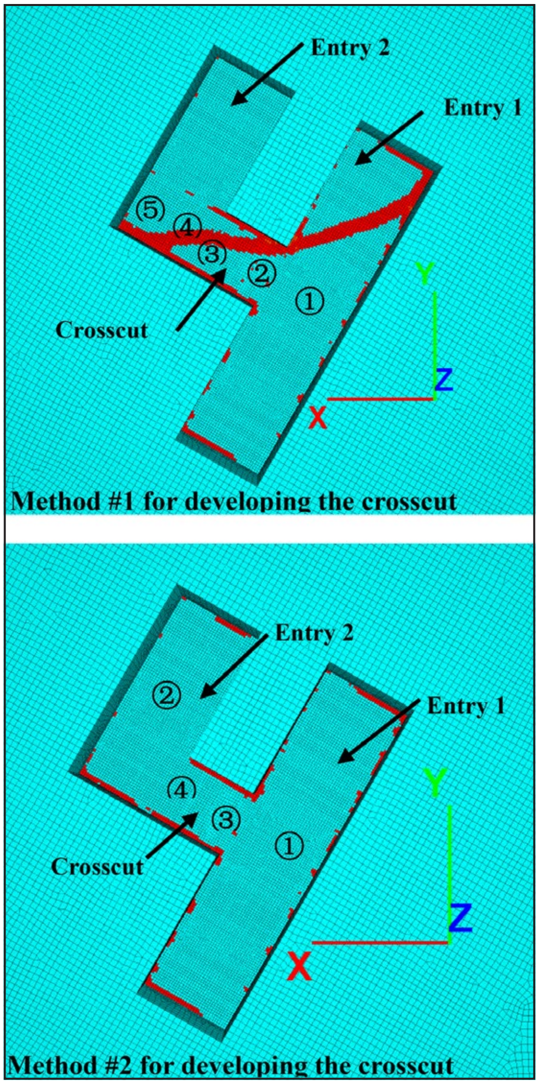

Figure 18. Yield pattern for a non-linear FLAC3D models of crosscut development using both the first and the second methods. Yielded elements are shown in red

creating a crosscut using the first method led to instability, while the second method produced a more stable crosscut. As illustrated in Figure 18, the yield pattern in the immediate roof from the FLAC3D model for the second method is significantly less than that of the first method. Therefore, it is recommended to develop new crosscuts using the second method when the roof is subjected to high horizontal stress.

Based on field observation, when the first method was used to create a crosscut, the crosscut was stable during the first three cuts however, when the last cut was done, the crosscut becomes unstable and cutter failure developed through it. Similar pattern was observed in FLAC3D model. However, it was found from the model that the crocsscut becomes unstable after excavating the third cut not the fourth cut as found from field observation. Field observations showed that when the first method was used, the crosscut remained stable during the first three cuts. However, instability and cutter failure developed after the final cut. The FLAC3D model displayed a similar pattern, although it indicated instability occurring after the third cut rather than the fourth, as observed in the field. Note that the direction of the maximum horizontal stress is parallel to the Y-axis.

SUMMARY AND CONCLUSION

Field observations from an operating mine and numerical models were used to assess the impact of maximum horizontal stress orientation, caprock thickness, face advance methods, and cutting sequences on roof stability. The key findings are as follows: when the caprock is thin and the roof is subjected to high horizontal stress, it is highly recommended to align entries parallel to the maximum horizontal stress to mitigate the detrimental effect of excessive horizontal stress. However, if the caprock is thick and massive, the influence of maximum horizontal stress on roof stability is less significant, even in unfavorable orientations, as increased caprock thickness reduces the induced shear stress in the roof above the excavation. Both field observations and numerical models suggest avoiding mining with an arrowhead front, as this method causes significant damage to all entries. In contrast, with a flat-front advance, only the outer entries were damaged. These findings enhance understanding of roof stability under high horizontal stress and contribute to reducing the risk of roof falls in underground stone mines. Additionally, preliminary evidence suggests enhanced stability when creating crosscuts by connecting existing entries to minimize instabilities caused by high horizontal stress.

LIMITATIONS OF THE STUDY

Many of the hazardous conditions in underground stone mines are the result of a complex interaction between geologic conditions and mining-induced factors. The conclusions drawn from the field observations in this study are inherently limited by the specific mining and geological conditions present at the study site, which may or may not be directly applicable to other mines with different characteristics. Variations in rock mass properties, stress regimes, and geological structures in other mines could lead to different outcomes.

Additionally, the results obtained from the FLAC3D models are constrained by the input parameters and the applied boundary conditions. While every effort was made to use realistic and representative values, uncertainties in material properties, stress distributions, and other input data could affect the precision of the model predictions. Therefore, the findings should be interpreted within the context of these limitations, and caution should be exercised when generalizing the results to other mining operations or geological settings.

DISCLAIMER

The findings and conclusions in this report are those of the author(s) and do not necessarily represent the official position of the National Institute for Occupational Safety and Health, Centers for Disease Control and Prevention. Mention of any company or product does not constitute endorsement by NIOSH.

REFERENCES

[1] Agapito, J. F. T., & Gilbride, L. J. (2002). Horizontal Stresses as Indicators of Roof Stability. *Proceedings of the 2002 SME Annual Meeting, Phoenix, Arizona, February 25–27*. Society for Mining, Metallurgy & Exploration.

[2] Chen, H. J. (1999) Stress Analysis in Longwall Entry Roof under High Horizontal Stress, Ph.D. dissertation, West Virginia University, pp 278.

[3] Esterhuizen, G. S., & Iannacchione, A. T. (2005). Effect of the dip and excavation orientation on roof stability in moderately dipping stone mine workings. In *Proceedings of the 40th U.S. Symposium on Rock Mechanics (USRMS)*, Anchorage, AK, USA, 25–29 June 2005.

[4] Evanek, N., Iannacchione, A., and Miller, T. (2020). Controlling Crosscut Damage in Response to Excessive Levels of Horizontal Stress: Case Study at The Subtropolis Mine, Petersburg, OH. *SME Annual Meeting, Phoenix, Arizona, February 23–26*. Society for Mining, Metallurgy & Exploration.

[5] Evanek, N., Rashed, G., Miller, T., Yeley, A., Klemetti, T. (2024) Principal Horizontal Stress Contributing to Massive Roof Collapse at the Subtropolis Mine. *SME Annual Meeting, Phoenix, Arizona, February 25–28*. Society for Mining, Metallurgy & Exploration.

[6] Gadde, M. M., and Peng, S. S. (2005) Numerical simulation of cutter roof failures under weak roof conditions, SME annual meeting 2005, Salt Lake City, Utah.

[7] Gale, W. J., and Blackwood, R. W. (1987) Stress distributions and rock failure around coal mine roadways, International Journal of Rock Mechanics, Mining Science and Geomechanics, Vol. 24, No.3, pp 165–173.

[8] Goodman, R. E. (1989). *Introduction to Rock Mechanics* (2nd ed.). John Wiley & Sons.

[9] Iannacchione, A. T., Dolinar, D. R., & Mucho, T. P. (2002). *High Stress Mining Under Shallow Overburden in Underground U.S.* Intern. Seminar of Deep and High Stress Mining, Australian Centre for Geomechanics, Section 32, Perth, Australia, Nov. 6–8, 2002, pp. 1–11.

[10] Iannacchione, A., Miller, T., Esterhuizen, G., Slaker, B., Murphy, M., Cope, N., and Thayer, S. (2020). Evaluation of stress-control layout at the Subtropolis Mine, Petersburg, Ohio, International Journal of Mining Science and Technology, Volume 30, Issue 1.

[11] Iannacchione, A.T., Dolinar, D.R., Prosser, L.J., Marshall, T.E., Oyler, D.C., & Compton, C.S. (1998). Controlling Roof Beam Failures from High Horizontal Stresses in Underground Stone Mines. In *Proceedings of the 17th International Conference on Ground Control in Mining*. Morgantown, WV: University of West Virginia, pp. 102–112.

[12] Iannacchione, A.T.; Marshall, Thomas E.; Prosser, Leonard J. 2001. Failure Characteristics of Roof Falls at An Underground Stone Mine In Southwestern Pennsylvania. Proceedings of the 20th International Conference on Ground Control in Mining, August 7–9, 2001, Morgantown, West Virginia. Peng SS, Mark C, Khair AW, eds., Morgantown, WV: West Virginia University, 2001 Aug; :119–125.

[13] Jaeger, J.C., Cook, N.G.W., & Zimmerman, R.W. (2007). Fundamentals of Rock Mechanics (4th ed.). Malden, MA: Blackwell Publishing. ISBN: 978-0632057597.

[14] Jeremic, M. L. (1981) Coal Mine Roadway Stability in Relation to Lateral Tectonic Stress-Western Canada, Mining Engineering, pp 704–709.

[15] Mark, C., & Gadde, M. (2010). Global trends in coal mine horizontal stress measurements. In N. Aziz (Ed.), *10th Underground Coal Operators' Conference* (pp. 21–39). University of Wollongong & Australasian Institute of Mining and Metallurgy.

[16] Mine Data Retrieval system. (2023). Mine Safety and Health Administration. Mine Data Retrieval System | Mine Safety and Health Administration (MSHA).

[17] Mogi, K. (2007). Experimental Rock Mechanics. London: Taylor & Francis. ISBN: 978-0415391031.

[18] Mucho, T. P., and Mark, C. (1994) Determining Horizontal Stress Direction Using Stress Mapping Technique, Proceeding of 13th International Conference on Ground Control in Mining, West

Virginia University, Morgantown, West Virginia, pp 277–289.

[19] Obert, L., and Duvall, W. I. (1967). *Rock Mechanics and the Design of Structures in Rock*. John Wiley & Sons.

[20] Peng, S. S. (2008). Ground Control Failures: A Pictorial View of Case Studies. Littleton, CO: Society for Mining, Metallurgy & Exploration. ISBN: 978-0873352620.

[21] Peng, S.S. (2007) Ground Control failures- a Pictorial view of case studies, S.S. Peng publisher.

[22] Peng, S.S. (2008) Coal Mine ground Control, 3rd Edition, S.S. Peng publisher.

[23] Ray, Anil Kumar, "Influence of cutting sequence and time effects on cutters and roof falls in underground coal mine -- numerical approach" (2009). Graduate Theses, Dissertations, and Problem Reports. 3491. https://researchrepository.wvu.edu/etd/3491.

[24] Sheorey, P.R., Murali Mohan, G., & Sinha, A. (2001). Influence of elastic constants on the horizontal in situ stress. *International Journal of Rock Mechanics and Mining Sciences*, 38(8), 1211–1216. https://doi.org/10.1016/S1365-1609(01)00069-7.

[25] Wang, Y., and Stankus, J. (1998) Roof Control Under Conditions of Shallow Depth and High Horizontal Stress Field - A Case Study, Proceedings of the 17th International Conference on Ground Control in Mining, West Virginia University, Morgantown, West Virginia, pp 113–118.